Int. J. Solids Structures Vol. 22, No. 9, pp. 985–1005, 1986
Printed in Great Britain

0020-7683/86 $3.00 + .00
Pergamon Journals Ltd

INITIATION AND PROPAGATION OF BUCKLES IN PIPELINES

T. WIERZBICKI and S. U. BHAT
Department of Ocean Engineering, Massachusetts Institute of Technology, Cambridge, MA 02139, U.S.A.

(*Received* 11 *March* 1985; *in revised form* 27 *June* 1985)

Abstract—Simple closed-form solutions are derived for the pressure necessary to initiate and propagate the buckle down the tube. The calculations are performed assuming that the dominant effect on the plastic energy dissipation has the circumferential bending mode. Using a rigid-plastic material idealization a simple moving hinge model which describes the deformation of a ring into a "dumbbell" shape is proposed. Strain-hardening effects are taken into account in an approximate way. The propagation pressure P_p is shown to be controlled by the thickness to diameter ratio of the shell and the ratio of the work-hardening modulus to the flow stress of the material. The resulting analytical solution for P_p is compared with the experimental results of Kyriakides *et al.* and the previous analytical solution due to Palmer and Martin. The solution for the initiation pressure P_i is derived on the basis of the same structural model in conjunction with a new conceptual model for buckle initiation. The derived solutions for both P_p and P_i are shown to correlate well with the experimental results recently reported in the literature.

NOTATIONS

a, b	numerical constants in eqn (22b)
f	function defined in eqn (7)
$g(m)$	minimum value of $F(x, y, m)$ for fixed m, Table 1
h	tube wall thickness
m	$\frac{1}{3}(E_p/\sigma_0)(h/D)$, strain-hardening parameter
n	exponent in eqn (34)
r	a geometric parameter defined in Fig. 5(b)
t	time
x	R_1/R
y	R_2/R
A	area enclosed within the collapsing tube
A_0	πR^2 = the initial value of A
A_f	final value of A
A^*	value of A corresponding to the idealized damaged section
D	tube diameter
D^*	Figure 5
E_{int}	internal (plastic) work for a unit length of tube
E_{ext}	external work done by the pressurizing medium
E	modulus of elasticity, eqn (34)
E_p	strain-hardening modulus
F	equation (21)
M_i	yield moment at the ith hinge, eqn (10)
M_0	$\sigma_0 h^2/4$
$M_{A'}, M_{B'}$	yield moments at moving hinges A' and B'
P	external pressure
P_p	propagation pressure
P_i	initiation pressure
P_c	buckling pressure
R	$D/2$, tube radius
R_1, R_2	radii of curvature of the deformed parts, Fig. 3
V	velocity of the traveling hinge in the tangential direction
Y	uniaxial yield stress according to the API definition
α, β	angles which describe the current position of the moving hinges, Fig. 3
α_f, β_f	values of α and β at touchdown
γ	exponent in $P_p/\sigma_0 = C(h/D)^\gamma$
ε	total engineering strain
ε^p	plastic strain
θ^*	Figure 5(a)
ξ	half-length of the straight line segments, Fig. 5(b)
σ	engineering stress
σ_0	uniaxial initial yield stress in the rigid linearly strain-hardening idealization
σ_y	uniaxial yield stress (0.2% offset)

κ change in meridional curvature
Ω angular velocity of an element of the ring for rotation in the plane of the ring
[ ] jump in the enclosed quantity across stationary or moving hinges
$(\cdot)$ $(\partial/\partial t)(\ )$, differentiation with respect to time
$(\ )^*$ quantity associated with a magnitude of damage given by D^*
K $1/R$, curvature (Section 10)

1. INTRODUCTION

The propagating buckle is a phenomenon in which an overall damage of large sections of pipelines takes place due to a catastrophic collapse of tube cross-sections under external pressure. The buckle is usually initiated from a local dent on a tube. Once initiated, the buckle propagates at high velocity flattening the pipe or cylindrical shell. This problem was first encountered in offshore pipeline applications. A proper understanding of the process of initiation, propagation and buckle arrest is of great importance to the offshore petroleum industry. A need for improved analysis of this problem is expected to continue in the future as the activities of exploration and exploitation of offshore mineral and oil deposits expand into deeper waters where external pressures are higher.

The minimum external pressure required to propagate a buckle down the pipe under steady, quasistatic conditions is called the propagation pressure, P_p. It is less than the initiation pressure P_I, which is the minimum pressure at which a dent or local damage will transform itself into a propagating buckle. Both P_p and P_I are usually much less than the buckling pressure P_c of perfect geometry shells under external pressure, for pipe sizes of interest in offshore applications. Palmer and Martin[1] gave one of the early accounts of the buckle propagation phenomenon. Mesloh *et al.*[2] conducted the first systematic experimental study of the problem using both small and full scale specimens. Kyriakides, Babcock *et al.*[3–5] have carried out extensive theoretical and experimental studies of a number of aspects of buckle initiation, propagation and arrest. Recently, Chater and Hutchinson[6] proposed a numerical procedure for estimating the propagation pressure, using the deformation theory of plasticity. Specifically, a plane strain ring model was used to estimate the energy dissipated in plastic deformation. Kyriakides *et al.*[7] used the same procedure, with minor changes, to predict the propagation pressure of some steel and aluminum alloy tubes.

In this article we apply the kinematic methods of plasticity to derive simple analytical solutions for the propagation and initiation pressures. The propagation pressure is calculated assuming that the dominant effect on the energy dissipation has the circumferential bending mode. Based on a rigid-plastic material idealization, a simple moving hinge model which describes the ring deformation to dumbbell shape is proposed. Strain-hardening effect is taken into account in an approximate manner. The resulting simple analytical solution for P_p is compared with the experimental results of Kyriakides *et al.* and the previous analytical solution due to Palmer and Martin. The solutions for the initiation pressure P_I are derived on the basis of structural models for ring deformation in conjunction with a new conceptual model for buckle initiation. The derived solutions for P_I are shown to correlate well with the experimental results reported in [5].

In an attempt to bring the theory closer to experiments, Croll[8, 9] extended Palmer's solution by incorporating the strain hardening of the material. However, his solution was based on a different kinematic model of the ring, and the resulting propagation pressure is smaller than in the present solution, especially for thicker tubes or larger work-hardening modulus. A detailed comparison of the present solution with that of Croll is presented in the last section of this article.

2. ANALYSIS OF THE EXTENSIBLE AND INEXTENSIBLE DEFORMATION MODELS

Under steady-state quasistatic conditions the work done by the pressure due to the consequent volume change is equal to the energy of deformation. Since the deformation is very large, plastic deformation dominates over the effects of elasticity. Palmer and Martin[1] assumed that the plastic energy dissipation is mainly in inextensional circumferential bend-

ing of the tube sections. Using a rigid-perfectly plastic material idealization, they estimated the plastic work of deformation in a ring model with four inextensional plastic hinges as shown in Fig. 1(a), and derived the following expression for propagation pressure

$$P_p = \pi\sigma_0(h/D)^2, \tag{1}$$

where σ_0 is the yield stress of the pipe material, h is the pipe thickness, and D is the diameter. Equation (1) is known to underestimate the propagation pressure, especially for steel pipes. Another drawback of this model is that it corresponds to a one-parameter material idealization. Experimental observations on steel and aluminum alloy pipes indicate that it is important to account for differences in strain hardening[3]. In this regard, it is interesting to note that strain-hardening effect was found to be significant in a related problem of lateral crushing of tubes between rigid plates[10].

Chater and Hutchinson[6] and Kyriakides *et al.*[7] also assumed that the dominant effect is the ring deformation mode. These authors calculated the plastic work of ring deformation numerically, assuming the appropriate relation for the uniaxial stress–strain behavior of the pipe material. Using accurate representation of the material stress–strain behavior, numerical results were obtained for the propagation pressures of a number of steel and aluminum alloy tubes.

The inextensibility of the tube generators imposes an important restriction on the mode of ring deformations. This can be best explained on a somehow simpler model of a square tube collapsing under an external pressure. Suitable models of such tubes made of construction paper are shown in Figs. 2(a) and (b), respectively. The model with stationary plastic hinges, Fig. 2(a), could not be constructed without precutting the paper. This means that there must be considerable shear and/or extensions present in this model. Moreover, it is easy to see that the lengths of the generators AA' and BB' are different which further support the conclusion about the shape distortion during buckle propagation.

An alternative model in which plastic hinges travel with respect to the material points is shown in Fig. 2(b). All generators are seen to be of equal length so that no axial deformation is produced during the buckle propagation process. It should be pointed out

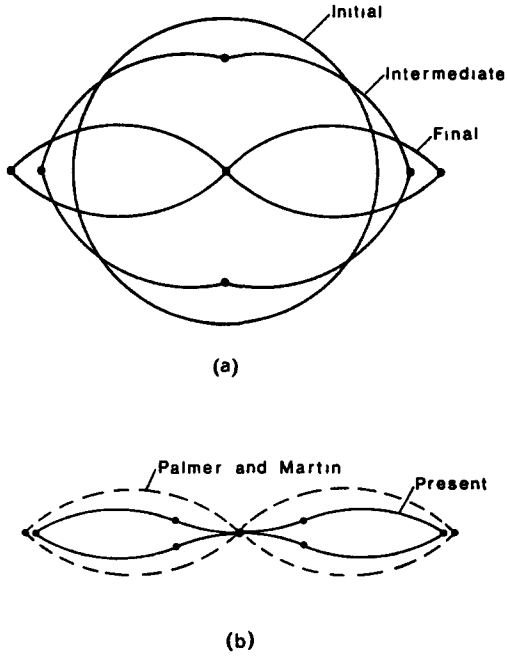

Fig. 1. (a) Stationary hinge ring model of Palmer and Martin. (b) Predicted final shapes of the collapsed tube made of a rigid-perfectly plastic material, (– – –) Palmer and Martin model, (——) present traveling hinge model (with $m = 0$).

that the model with traveling plastic hinges represents the motionless configuration, where slope discontinuities are allowed. In the same model set into motion, the slope discontinuities would vanish giving rise to a smooth cross-sectional shape.

The above discussion indicates that a consistent model of the propagating buckle should include the following deformation modes:

(1) Bending of rings at stationary plastic hinges plus extensions of the generators, or
(2) Bending (and rebending) of rings at moving plastic hinges but no extension of tube generators.

The difficulty in proceeding with the first possibility is the fact that the amount of axial extension depends on the length of the transition zone between the initial circular and collapsed section. This length cannot be determined from the theory of steady-state buckle propagation.

Here we shall explore the second possibility. For circular tubes the conclusion that the generators are fully inextensible is not true, but our preliminary calculations indicate that the longitudinal strains are likely to be within the elastic range, except for very low values of D/h. In recent years the theory of traveling hinges has been successfully applied in the analysis of numerous practical problems in which deformations are large and highly localized (see for example [11–13], etc.). This theory will now be used to construct a structural model for the ring deformations which closely resembles the actual shapes observed experimentally and leads to a simple closed-form solution.

Our traveling hinge model for the ring deformation is based on the rigid-linearly strain hardening idealization of material uniaxial stress–strain behavior. The ring is assumed to undergo inextensional deformation from the initial circular shape to a final dumbbell shape. The shapes of a collapsing ring at various stages of collapse (as per the proposed model) are shown in Fig. 3. Initially, four equispaced hinges form on the circular ring, as in Palmer's model. However, in contrast to Palmer's model, we allow the hinges to move with respect to material points. As the deformation progresses, each of these plastic hinges splits into two hinges traveling in opposite directions. A hinge or hinge-line moving down an undeformed surface leaves behind a deformed surface[11]. For simplicity, we assume that the deformed parts of the ring are also of constant curvature. The model assumes that the central hinges (such as A') leave behind a region of constant curvature $-1/R_1$, and the side hinges (such as B') leave behind a region of constant curvature $1/R_2$. Due to the symmetry, deformation behavior of the four quadrants of the ring is identical. The kinematics of one of the quadrants (AB) is shown in Fig. 3(b). The point A' shown in Fig. 3(b) represents the current position of one of the moving hinges which originated at the material point A (similarly B'). As the deformation proceeds, the length of the undeformed portion of this segment, $A'B'$, diminishes while the lengths of the deformed portions, AA' and BB', increase. In view of the inextensibility assumption, the total perimeter of the ring remains constant. For one quadrant

$$\alpha R_1+\beta R_2+R(\pi/2+\alpha-\beta)=\pi R/2, \tag{2}$$

where α and β are angles shown in Fig. 3, and R is the initial mean radius of the circular tube. Equation (2) can be nondimensionalized to give

$$\alpha(1+x)=\beta(1-y), \tag{3}$$

where

$$x=R_1/R \qquad \text{and} \qquad y=R_2/R. \tag{4}$$

It may be noted that the nondimensional radii x and y are assumed to remain constant during the deformation process. Since α and β are related by eqn (3), any one of the two radii may be taken to be the independent time-like parameter which describes the process of deformation. In the following, we will take α to be the time-like parameter.

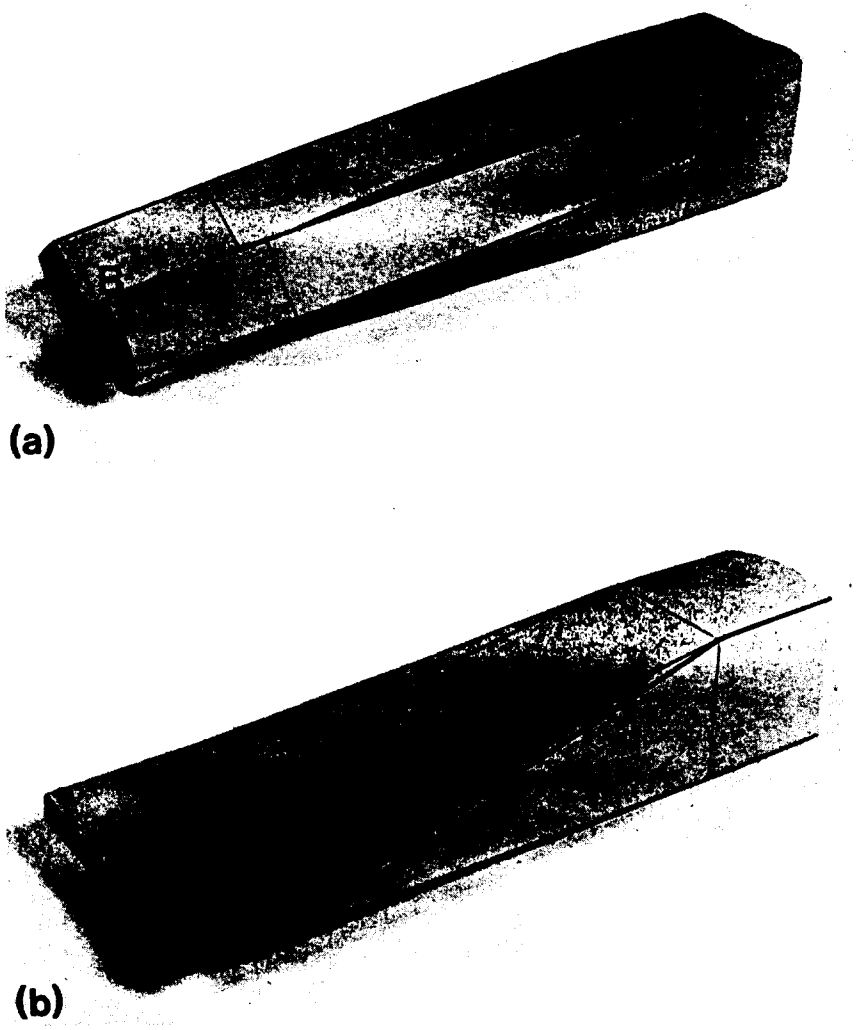

Fig. 2. Photographs of construction paper models for the propagating collapse of a square tube, (a) a stationary hinge model, (b) a traveling hinge model.

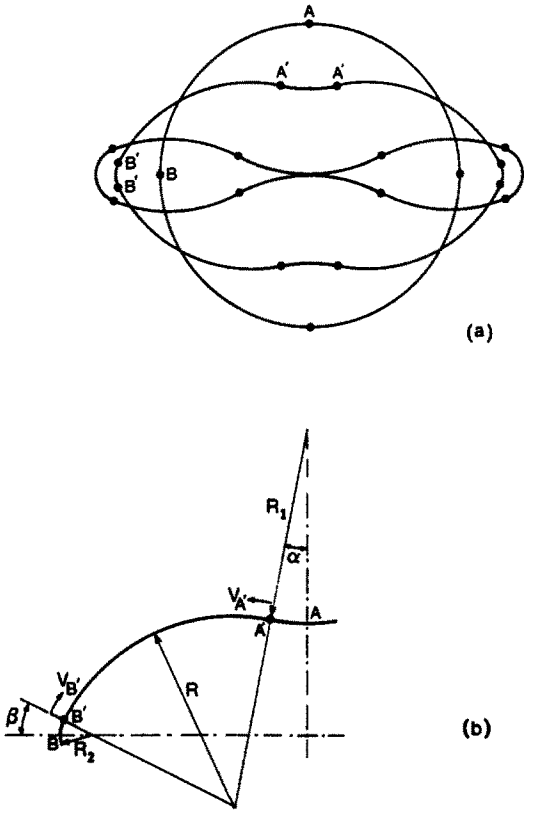

Fig. 3. The proposed traveling hinge model for ring deformation, (a) the initial, intermediate, and final shapes of a deforming ring, (b) details of the kinematics of deformation.

Touching of the two opposite quarter points occurs when $\alpha = \alpha_f$. The geometric condition for touching can be put as

$$(1+x)\cos\alpha_f-(1-y)\sin\left\{\left(\frac{1+x}{1-y}\right)\alpha_f\right\}-x-\frac{h}{D}=0, \tag{5}$$

where eqn (3) has been used to eliminate β_f, which is the final value of β.

The area enclosed by the collapsing tube A at a current value of the parameter α is

$$A(\alpha)=\pi R^2-2R^2f(\alpha), \tag{6}$$

where

$$f(\alpha)=\left[\left(\frac{x+y}{1-y}\right)\alpha+(1-y)^2\sin^2\left\{\frac{1+x}{1-y}\alpha\right\}\left[\tan\alpha+\cot\left\{\frac{1+x}{1-y}\alpha\right\}\right]\right.$$
$$\left.+x^2\alpha-y^2\left(\frac{1+x}{1-y}\right)\alpha-\left\{(1+x)\cos\alpha-(1-y)\sin\left(\frac{1+x}{1-y}\alpha\right)\right\}^2\tan\alpha\right]. \tag{7}$$

The area is seen to diminish from the initial value at $\alpha = 0$, $A_0 = A(0) = \pi R^2$ to its final value $A(\alpha_f) = A_f$. The current nondimensional reduction and the maximum reduction of the enclosed area are defined respectively by

$$[A_0-A(\alpha)]/R^2=2f(\alpha), \qquad (A_0-A_f)/R^2=2f(\alpha_f). \tag{8a, 8b}$$

The rate of work of external pressure $\dot{E}_{ext}$ is

$$\dot{E}_{ext} = -P\dot{A} = -P2R^2 \frac{df(\alpha)}{d\alpha}\dot{\alpha}, \tag{9a}$$

where a dot denotes differentiation with respect to time. If the external pressure P is constant, then the total external work in collapsing a ring to touchdown is

$$E_{ext} = \int_0^{t_f} \dot{E}_{ext}\, dt = P(A_0 - A_f). \tag{9b}$$

3. CALCULATION OF INTERNAL ENERGY DISSIPATION

Let us consider collapse of a ring of unit length in the axial direction. According to the kinematics of our model, plastic dissipation is restricted to the moving hinges only; there is no continuously deforming region. The time rate of internal dissipation is

$$\dot{E}_{int} = \sum_{i=1}^{8} |M_i[\Omega]_i|, \tag{10}$$

where M_i is the yield moment of the tube wall at the ith hinge, and Ω is the angular velocity of an element of the ring for rotation in the plane of the ring. The symbol [ ] denotes a jump in the corresponding quantity across stationary or moving hinges. Conditions for kinematic continuity at moving hinge-lines on shells were discussed by Abramowicz and one of the present authors[11]. In the present case, these conditions reduce to the following, at each traveling hinge

$$[\Omega] + V[\kappa] = 0, \tag{11}$$

where κ is the circumferential curvature, and V is the velocity of the traveling hinge in the tangential direction.

Making use of the symmetry of our model and eqn (1) with the appropriate values of jumps in curvature across the moving hinges A' and B', we may write eqn (10) as follows:

$$\dot{E}_{int} = 4\left\{M_{A'}V_{A'}\left(\frac{1}{R} + \frac{1}{R_1}\right) + M_{B'}V_{B'}\left(\frac{1}{R_2} - \frac{1}{R}\right)\right\}, \tag{12}$$

where $M_{A'}$ and $M_{B'}$ are the plastic yield moments, and $V_{A'}$ and $V_{B'}$ are the tangential velocities corresponding to the traveling hinges A' and B', respectively. It is to be understood that both terms on the right-hand side of eqn (12) are nonnegative. The tangential velocities of the moving hinges are given by

$$V_{A'} = R_1\dot{\alpha}, \tag{13a}$$

$$V_{B'} = R_2\dot{\beta} = R_2\left(\frac{1+x}{1-y}\right)\dot{\alpha}. \tag{13b}$$

We incorporate the strain-hardening effect in our model by relating the plastic yield moments $M_{A'}$ and $M_{B'}$ to the changes in curvature introduced by the corresponding traveling hinges A' and B', respectively. For a rigid-linearly strain-hardening material, the moment curvature relation for continued bending without strain reversal is

$$M = M_0 + (E_p h^3/12)\kappa, \tag{14}$$

where $M_0 = \sigma_0 h^2/4$, κ is the change in curvature, and σ_0 is the uniaxial yield stress of our rigid-linearly strain-hardening idealization. It is assumed that the material obeys the Tresca yield condition, therefore, the yield stress for yielding in the circumferential direction is the same as the uniaxial yield stress for both plane stress and plane strain ring deformations.

Substituting $\kappa = 1/R + 1/R_1$ for hinge A' and $\kappa = 1/R_2 - 1/R$ for hinge B' in eqn (14), we obtain

$$M_{A'} = M_0\{1+2m(1+1/x)\}, \tag{15a}$$

$$M_{B'} = M_0\{1+2m(1/y-1)\}, \tag{15b}$$

where

$$m = \tfrac{1}{3}(E_p/\sigma_0)(h/D). \tag{16}$$

Using the results of eqns (13) and (15) in eqn (10), we get the rate of internal dissipation

$$\dot{E}_{\text{int}} = 8M_0\{1+m(1/x+1/y)\}(1+x)\dot{\alpha}. \tag{17}$$

The total energy dissipated in plastic work can be obtained by integrating eqn (17):

$$E_{\text{int}} = \int_0^{t_f} \dot{E}_{\text{int}}\, dt = 8M_0\{1+m(1/x+1/y)\}(1+x)\alpha_f, \tag{18}$$

where t_f is the time at completion of collapse. We assume that collapse is completed when the first touchdown occurs. (Subsequent elastic spring back effects are of course neglected.) This assumption was also made by Chater and Hutchinson[6] who justified it on the basis of experimental observations of Kyriakides.

4. DETERMINATION OF THE PROPAGATION PRESSURE

The instantaneous pressure necessary to deform the ring can be calculated by equating the external and internal rate of energy dissipations, $\dot{E}_{\text{int}} = \dot{E}_{\text{ext}}$, eqns (9a) and (17). From the form of these equations it can be seen that the external pressure required to initiate deformation on a rigid-plastic perfect ring is infinite. (This pressure will be finite and limited to the elastic or elastic-plastic buckling pressure, if the elastic effects are included.) The pressure required to progressively deform the ring falls steeply as the deformation progresses.

As the buckle propagates down the tube, each ring of a unit width undergoes the entire history of the deformation process from an initial circular shape to the final shape determined by the terminal value of the parameter $\alpha = \alpha_f$.

The equation for determining the quasistatic propagation pressure P_p under steady-state conditions has to be obtained from the energy balance requirement that the work done by P_p in collapsing the ring (or a unit length of tube) to its final dumbbell shape must equal the total internal energy dissipated. Using eqn (9b) for E_{ext}, energy balance gives

$$P_p(A_0 - A_f) = E_{\text{int}}. \tag{19}$$

Equation (19) can be interpreted to mean that the propagation pressure is the average pressure under which a ring will be crushed to the final dumbbell shape. That is, it may be conceived to be the pressure corresponding to the "Maxwell Line" of the pressure versus reduction in area curve[6].

Substituting the results of eqns (8) and (18) into eqn (19), we obtain

$$P_p = F\sigma_0(h/D)^2, \tag{20}$$

Table 1

m	x_{opt}	y_{opt}	α_f (rad)	$g(m) = F(m)_{min}$
0	1.095	0	0.441	3.01
0.02	0 95	0.15	0.492	3.80
0.04	1.01	0.19	0.489	4.26
0.06	1.05	0.21	0.491	4.68
0.08	1.07	0.22	0.493	5.07
0 10	1.09	0.23	0.494	5.45

where the function F is given by

$$F = (4/f)\{1+m(1/x+1/y)\}(1+x)\alpha_f, \tag{21}$$

where f is defined in eqn (7).

It seems reasonable to assume that $x \gg h/D$, and therefore the term h/D can be dropped from the touching condition of eqn (5). Then eqn (5) can be used to solve for α_f, given x and y. That is, $\alpha_f = \alpha_f(x, y)$. Therefore, $f = f(x, y)$, and consequently $F = F(x, y, m)$.

We postulate that the steady-state propagation pressure P_p will be a minimum with respect to the parameters x and y which describe the shape of the collapsing tube. Similar postulates have been successfully used in problems of crushing mechanics (see, for example [11]). Indeed, for fixed values of m, the minimum of the function F does exist with respect to both x and y. A short computer program was written to perform this minimization computation and the results are provided in Table 1. In Table 1, the minimum of $F(x, y, m)$ at a fixed value of m is denoted by $g(m)$. The following equation adequately approximates the function $g(m)$ in the range of interest†

$$g(m) = 3+12m^{0\,7}. \tag{22a}$$

Equation (22a) has been obtained by fitting a curve of the type

$$g(m) = g(0)+am^b, \tag{22b}$$

where a and b are numerical constants to be determined, to the values of $g(m)$ given in Table 1, by least squares method. The constant term 3.0 is obtained from the consideration of the limiting case of rigid-perfectly plastic material (see the next section). Equation (20) now gives

$$P_p = g(m)\sigma_0\left(\frac{h}{D}\right)^2 \cong \left\{3+12\left(\frac{1}{3}\frac{E_p}{\sigma_0}\frac{h}{D}\right)^{0.7}\right\}\sigma_0\left(\frac{h}{D}\right)^2, \tag{23}$$

where we have used the definition of m from eqn (16).

5. PROPAGATION PRESSURE FOR THE SPECIAL CASE OF RIGID-PERFECTLY PLASTIC MATERIAL

The present analysis contains Palmer's solution as a special case. Palmer assumed stationary hinges and neglected the thickness in formulating the touching condition. Equivalently, substituting $x = y = h = 0$ in eqn (5), we get $\alpha_f = \pi/4$. Substitution of these values in eqn (7) provides $f = 1$. For a rigid-perfectly plastic material, $m = 0$, and therefore $F = \pi$ from eqn (21), since the term which represents the strain-hardening effect goes to zero. Equation (20) thus reduces to Palmer's solution given by eqn (1).

† The exact calculated value of $g(0)$ is 3.01, and the numerical values of a and b obtained are 12.07 and 0 70, respectively. We are suggesting the rounded up values for practical applications.

However, for a rigid-perfectly plastic material, the hinges do not necessarily have to be stationary. In the limiting case of $m = 0$, eqn (20) reduces to

$$P_p \simeq 3\sigma_0(h/D)^2, \tag{24}$$

which is close to eqn (1), but not exactly the same. This is so because $x_{opt} \neq 0$ for $m = 0$, although $y_{opt} = 0$ (see Table 1). Consequently, the shapes of collapsed tube at touchdown corresponding to eqns (1) and (24) are quite different [Fig. 1(b)]. The present analysis predicts larger reduction in the enclosed area than Palmer's analysis. The plastic work of deformation is also larger, but not large enough to raise the value of F to π.

6. PREDICTION OF WET BUCKLES

The present theory may be used to get an estimate of the maximum strain in the pipe due to a propagating buckle. Information regarding the maximum strain can be useful in predicting the so-called "wet buckle" which may result from a propagating buckle. Wet buckle is the name given to any kind of severe damage to an offshore pipeline which has caused rupture that led to flooding of pipeline[14]. Wet buckles are very undesirable because they require dewatering and cleaning up processes (the ruptured underwater pipeline may get filled up by dirt) which are very time consuming and consequently very costly.

The maximum (circumferential bending) strain is given by

$$\varepsilon_{max} = \left(\frac{1}{R_2} - \frac{1}{R}\right)\frac{h}{2} = \frac{h}{D}\left(\frac{1}{y} - 1\right), \tag{25}$$

where $y = R_2/R$ is a function of the parameter m as given in Table 1. An approximate fit to this function is

$$y = 0.4326m^{0.265}. \tag{26}$$

Using eqns (25) and (26),

$$\varepsilon_{max} = \frac{h}{D}\left\{2.31\left(\frac{1}{3}\frac{E_p}{\sigma_0}\frac{h}{D}\right)^{-0.265} - 1\right\}. \tag{27}$$

Equation (27) could be used together with an appropriate critical strain ductile fracture criterion, to predict the possibility of a wet buckle during quasistatic buckle propagation. Simplified approaches such as this have been successful in predicting the plastic failure of ductile beams[15] and were recently applied to the rupture analysis of ship plating[16].

7. PREDICTION OF THE INITIATION PRESSURE FOR DAMAGED PIPES

For a propagating buckle to occur it is necessary that the buckle be initiated from a local damage or dent in the pipe. The possible causes of local damage in a marine environment are numerous (see, for example, [17, 18]). In this section we limit our consideration to a particular situation: buckle initiation from a local denting damage which may be caused by external objects impacting on the pipe. The initiation pressure P_I is the minimum pressure at which the dent would grow and transform itself into a propagating buckle. Clearly, the shape and magnitude of the dent, as well as the material and geometric parameters of the pipe, influence the value of P_I. An exact treatment of this elastic-plastic shell instability problem would be exceedingly complex, even if particular dent geometries are assumed. A satisfactory solution for P_I would provide the marine industry with a way to estimate whether a given damage on a pipeline has the potential of being an initiation point for a propagating buckle.

Kyriakides and Babcock[5] have recently reported an extensive experimental investigation of this problem. They found that their experimental data for the initiation pressure could be coalesced if the initiation pressure was normalized by the propagation pressure and the damage was characterized by the dimensions of the most damaged section. This has motivated us to propose the following simple theory for buckle initiation, on the basis of which simple formulae for P_i/P_p can be derived in terms of dimensions of the most damaged section.

We hypothesize that the initiation pressure corresponding to a given dent size [characterized by D^*/D of the most damaged section (see inset in Fig. 10)] is equal to the average pressure which can theoretically propagate the damage down the pipe *thus increasing the extent of damage lengthwise* (Fig. 4). This pressure is presumed to be sufficient to deepen the dent too and subsequently lead to a full collapse of the tube.

The dent is actually deepened during the process of buckle initiation and deepening of the dent involves extension and shear of tube generators. A rigorous formulation of the buckle initiation problem should include these effects. We are overcoming this difficulty by proposing the simple conceptual model according to which buckle initiation can be understood as buckle propagation in a tube with partial closure. It is already known that extension/shear effects are small in the buckle propagation problem.

The damaged state is the state A in Fig. 4. We are applying a small incremental displacement field so that the neighboring state B is reached. Internal energy dissipation is only due to the ring crushing mode. The rate of external work can be computed by multiplying the pressure by the change in volume. However, the "Maxwell Line" argument is not applicable here, because the tube cannot be in a state of another stable equilibrium in the absence of touching. Instead we can use the work balance postulate, $E_{int} = E_{ext}$. Because the tube is not in a state of stable equilibrium, it is conjunctured that the pressure P_i calculated from the above equation will lead to the full collapse of the cross-section.

The shape of the most damaged section is now approximated by a suitable structural model of deforming ring. Palmer's model [Fig. 1(a)] or our traveling hinge model (Fig. 3) or any other suitable model could be used for this purpose. We first illustrate the approach using Palmer's stationary hinge model. Correspondingly, the pipe material is now assumed to be rigid-perfectly plastic. For a damaged section approximated by the stationary hinge model as shown in Fig. 5(a) it can be shown from the geometry that the minimum diameter of the damaged tube is related to the corresponding rotation angle of the rigid segments θ^* by

$$D^*/D = 1-\sin(\pi/4-\theta^*). \tag{28}$$

The area enclosed within the idealized damaged section is then

$$A^* = (\pi-2+2\sin 2\theta^*)R^2. \tag{29}$$

The internal plastic work dissipated in deforming a unit length of pipe to the damaged configuration represented by D^*/D or angle θ^* is

$$E_{int} = 8M_0(\pi/4-\theta^*). \tag{30}$$

Therefore, by energy balance, the minimum pressure required to propagate damage of this size is given by $E_{int}/(\pi R^2-A^*)$. This is taken to be the initiation pressure corresponding to

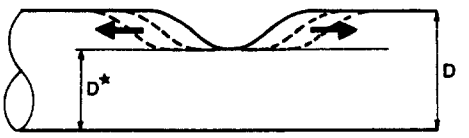

Fig. 4. Spreading of damage along the length of tube.

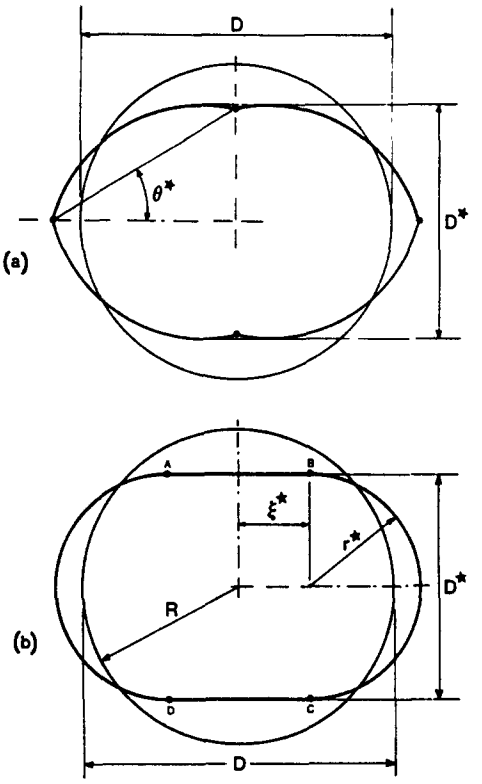

Fig. 5. Ring models used to predict initiation pressure.

the assumed damage size. Using (29) and (30), we obtain

$$P_I = \frac{4M_0}{R^2} \frac{(\pi/4 - \theta^*)}{(1 - 2\sin\theta^*)}. \tag{31}$$

The propagation pressure for this model is given by eqn (1). Using eqns (1), (28) and (31),

$$\frac{P_I}{P_p} = \frac{2}{\pi} \frac{\arcsin(-D^*/D)}{(1 - D^*/D)^2}. \tag{32}$$

The singularity at $D^* = D$ (perfect pipe) is due to the rigid-plastic idealization. In reality P_I will be bound by P_c, the elastic or elastic-plastic buckling pressure of the perfect pipe.

Our traveling hinge model of Fig. 3 is too complicated to lead to a simple closed form result [such as eqn (32)] for P_I. Another simpler moving hinge model for ring crushing is shown in Fig. 5(b). Again, the material is assumed to be rigid-perfectly plastic, to keep the analysis simple. The details of analysis corresponding to this model are given in Appendix A. The final result is

$$\frac{P_I}{P_0} = 0.41 \frac{\ln(D/D^*)}{(D/D^* - 1)^2}, \tag{33}$$

which also has a singularity at $D^* = D$. These predictions can further be improved by incorporating the elastic or elastic-plastic buckling effects which cannot be neglected when $D^*/D \simeq 1$.

An attempt to analytically predict the initiation pressure was made recently by Tam and Croll[19]. They used energy balance in a small incremental plastic deformation about the damaged state assuming that the incremental displacement field will be in a certain shape. The displacement increments were in terms of an increase in the depth of the dent.

They also neglected the contribution of extensional and shear effects to the incremental energies. But the justification for this assumption in their approach is, however, not clear from their paper. According to the calculations presented in [20], the extensional energy associated with the increase of the depth of the dent contributes to one-half of the total energy dissipated. A plastic mechanism analysis of tube damage was also presented in [19] as a precursor to their analysis of buckle initiation. The displacement field was assumed to be in a "mode form" but the final results for the load-response behavior indicate that this particular assumption is not valid. It is of interest to note that a similar problem arises in the analysis of rigid-plastic structures on foundations[21]. Rigorous solutions for these problems involve changing shapes of incremental displacement fields[22].

8. COMPARISON WITH EXPERIMENTAL DATA

Experimental results for the propagation pressures of stainless steel and aluminum alloy pipes of various sizes are given in [7]. All tubes tested by the authors of [7] were drawn and seamless. The aluminum alloys used were mainly 6061-T6, 6061-T4 and 2024-T3. The majority of steel tubes tested were stainless steel 304 with various heat treatments and a few 1018.

To compare our analytical result for the propagation pressure [eqn (23)] with the experimental data, we need to determine the mean value of E_p/σ_0 for each material family (steel and aluminum alloys). These values were not explicitly reported in [7]. An experimental stress–strain curve for SS-304 material of the stainless steel pipes tested by Kyriakides *et al.* was, however, given in [7]. This curve is shown in Fig. 6 along with out linear strain-hardening approximation, from which the value of E_p/σ_0 is calculated to be 4.87. It should be noted that the yield stress σ_0 of our linear strain-hardening idealization is different from the yield stress σ_y determined using the customary 0.2% offset strain criterion, which is also shown in Fig. 6. Kyriakides *et al.*[7] used σ_y to normalize their experimental data on the propagation pressure of stainless steel pipes. Our analytical result for P_p/σ_y follows directly from eqn (23), since $P_p/\sigma_y = (\sigma_0/\sigma_y)(P_p/\sigma_0)$. Using $\sigma_0/\sigma_y = 1.09$ (from Fig. 6) and $E_p/\sigma_0 = 4.87$, our eqn (23) is compared with the experimental results for stainless steel pipes, in Fig. 7. Also shown in Fig. 7 are the numerical solution of Kyriakides *et al.* and the Palmer and Martin solution, eqn (1), assuming the same value of σ_0/σ_y.

An approximate fit to the experimental uniaxial stress–strain curves of some of the AL-6061-T6 pipes tested by Kyriakides, was given in Ref. [6] as (Fig. 8)

$$\varepsilon = \sigma/E + (0.005 - Y/E)(\sigma/Y)^n, \tag{34}$$

where $E = 6.9 \times 10^4$ MPa, with $Y/E = 0.0042$ and $n = 30$. Here Y is the yield stress of the material determined according to the API definition of yield stress (Y = stress at $\varepsilon = 0.005$).

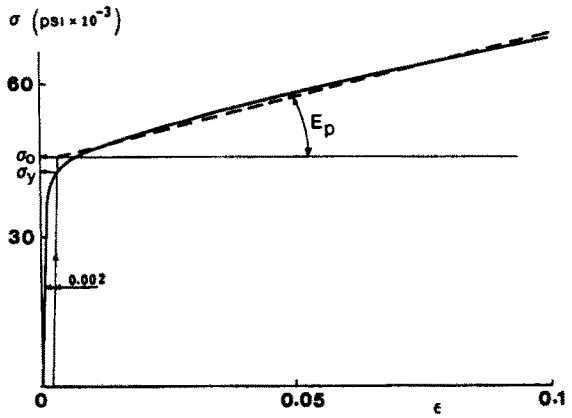

Fig. 6. Experimental stress–strain curve for SS-304 (Kyriakides *et al.*[7]) (solid) and our linear strain-hadening approximation (broken line).

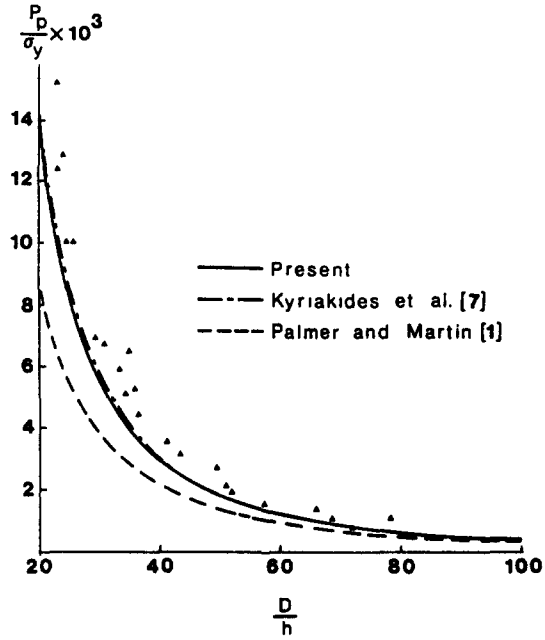

Fig. 7. Comparison of the theoretical and experimental results for the propagation pressure of stainless steel pipes. The experimental points (denoted by ▲) are taken from [7].

Equation (34) is plotted in Fig. 9 along with our linear strain-hardening approximation which is valid in the range of interest of plastic strain, $0 < \varepsilon^p < 0.1$. The values of σ_0 and E_p are determined to be 320 and 210 MPa, respectively, which give $E_p/\sigma_0 = 0.66$. The ratio σ_0/Y comes out to be 1.1. Kyriakide's experimental values of P_p/Y for aluminum alloy tubes were also reported in [6]. These test results are compared with our eqn (23) in Fig. 9, where we have made use of the relation $P_p/Y = (\sigma_0/Y)(P_p/\sigma_0)$ to obtain the solution for P_p/Y from eqn (23). Also shown in Fig. 9 are the numerical solution of Chater and Hutchinson, and the Palmer and Martin solution [eqn (1)] assuming the same value of σ_0/Y.

It is seen that the present solution for the propagation pressure correlates well with the experimental data, in the considered range of D/h. Palmer and Martin's solution is significantly lower than the present solution in the case of the stainless steel pipes. For the aluminum alloy pipes the difference between the two solutions is not large, since the material has low strain-hardening. The theoretical results are, in the main, somewhat lower

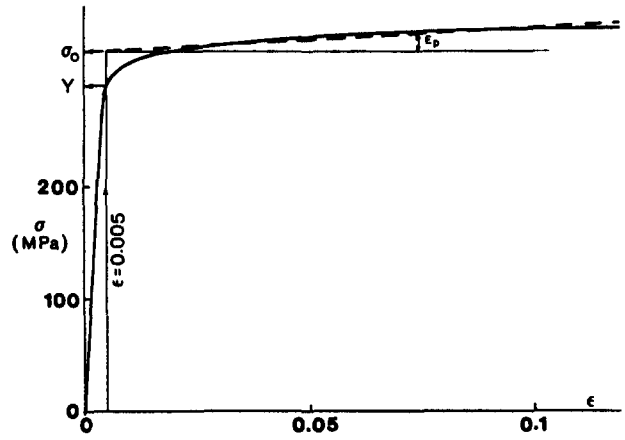

Fig. 8. Chater and Hutchinson's fit to the experimental stress–strain curves of AL-6061-T6 pipes tested by Kyriakides (solid line), and our linear strain-hardening approximation (broken line).

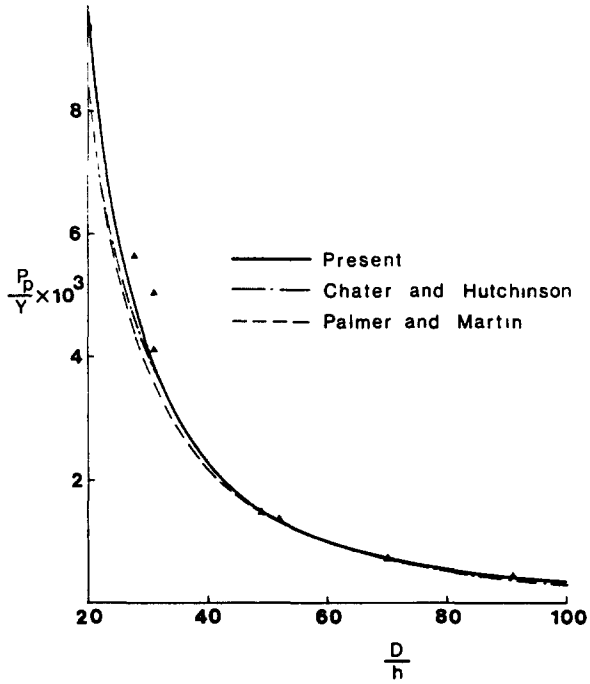

Fig. 9. Comparison of the theoretical and experimental results for the propagation pressure of aluminum alloy pipes. The experimental points (denoted by ▲) are taken from [6].

than the experimental ones. As noted in [7], this is attributable to the fact that only deformations of the cross sections were considered in energy balance.

In Fig. 10 we compare the present analytical results for the initiation pressure normalized with respect to the propagation pressure, eqns (32) and (33), with the experimental data reported in [5]. The pipes used in these experiments were made of steel. The initial denting damage was inflicted on the pipes using a knife edge indenter or a point indenter. It is seen that the theoretical predictions correlate reasonably well with the experimental data, considering the approximate nature of the theory and the fact that the theoretical initial damage shapes were symmetric while the experimental ones were unsymmetric.

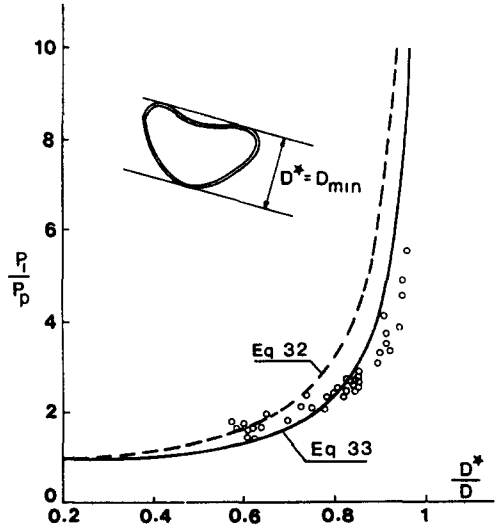

Fig. 10. Comparison of the theoretical predictions for P_i/P_p with the experimental data of Kyriakides *et al.* [5].

9. DISCUSSIONS AND CONCLUSIONS

The article presents our analytical solution for the propagation pressure P_p, which is the minimum external pressure causing the buckle to propagate once it has been initiated. This pressure is especially significant since at any pressure below P_p buckles cannot propagate, while at any prescribed pressure above P_p, the buckle (once initiated) will run dynamically, collapsing the entire length of pipe. The present solution describes the main features of the problem. The solution is constructed on the basis of a ring deformation model which uses the concept of traveling hinges. Strain-hardening effect is included in an approximate manner. The final result for the propagation pressure is given by eqn (23) which was shown to correlate well with the experimental data of Kyriakides *et al.* (Figs. 7 and 9).

The present solution is a significant improvement on the previous analytical solution due to Palmer and Martin in the sense that the strain-hardening effect (which is significant for tubes made of materials such as steel) is included in the solution. Also, the deformed shape of the tube resulting from our moving hinge model resembles very closely the "dog-bone" shape observed in practice.

The formula (23) contains two terms in the variable h/D. For the stainless steel 304, and the ratio $E_p/\sigma_0 = 4.87$, the normalized propagation pressure is given by

$$P_p/\sigma_0 = 3(h/D)^2 + 16.84(h/D)^{2.7}. \tag{35}$$

Several authors in the past including Mesloh *et al.*[2] and Kyriakides and Babcock[3] observed that a single power law $P_p/\sigma_0 = C(h/D)^\gamma$ with $\gamma = 2.25/2.5$ gave a fairly good approximation to the propagation pressures in a certain range of h/D. The present solution offers an explanation of this observation since the exponent γ is seen to lie somewhere between 2 and 2.7.

The predicted results are, in the main, lower than the experimental ones. This is attributable to the fact that only deformations of cross sections are considered in energy balance. For very thick tubes, thick wall effects and large strain effects may prevail. Moreover, our simplified analysis neglected the effect of the thickness on the touching condition. Therefore, the present solution is not expected to be accurate for $D/h < 20$.

It should be emphasized that the numerical solutions of the ring deformation problem do not lead to results that are any closer to experimental points than the present analytical prediction. The present paper also includes theoretical solutions of an approximate nature for the initiation pressure normalized with respect to the propagation pressure (P_i/P_p). These solutions [eqns (32) and (33)] correlate reasonably well with the experimental data reported in [5].

In addition to the above results the paper suggests a simplified approach to quantify the initiation of rupture in a pipeline during a quasistatic buckle propagation.

A unique feature of the present traveling hinge method is a possibility of extending the solution to the case of buckle propagation in a confined medium. The stationary hinge solution is inapplicable in this case while the numerical solution would require the treatment of the contact phenomena. The expression for the confined buckle propagation pressure will be derived in a future publication.

10. COMPARISON WITH THE SOLUTION BY CROLL

After the present work was completed, the authors came across an interesting paper by Croll[8] presented at the Offshore Mechanics and Arctic Engineering Symposium in Dallas, February 17–21, 1985. Since the objective of these two articles is similar, it will be instructive to compare the present approach with that used by Croll. In both approaches, the deformed shape of the ring consists of a system of arcs with various radii, so that the dog-bone shape of the buckle is well reproduced. However, the deformation process to reach the same final state is different in the two solutions.

In order to show the similarities and differences in the corresponding plastic work calculations, consider a section of an inextensible ring of the initial radius R_0 and arc length

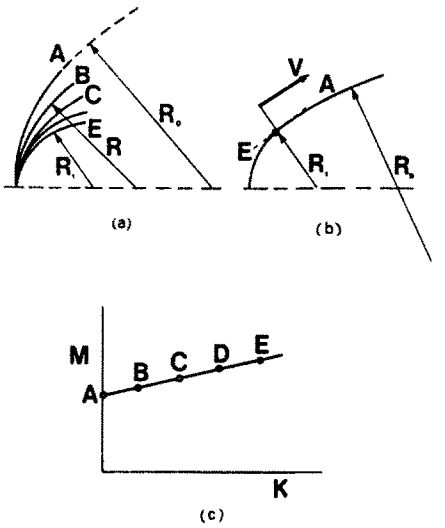

Fig. 11. Comparison of the present strain-hardening model with that of Croll.

$\mathscr{L}$. The ring is brought to a smaller final radius R_1 so that the final value of the central angle α_1 is given by $\mathscr{L} = R_1\alpha_1$ (Fig. 11).

In Croll's analysis[8], it was assumed that the final state is reached by gradually decreasing curvature of the arc from $K_0 = 1/R_0$ to $K_1 = 1/R_1$. The rate of energy dissipation in the continuous deformation field is

$$\dot{E} = \int_{\mathscr{L}} M\dot{K}\,\mathrm{d}l = \mathscr{L}M\dot{K}, \tag{36}$$

where $\mathrm{d}l$ is the increment of the arc length. The total plastic energy is a time integral of eqn (36):

$$E = \int_0^{t_f} \dot{E}\,\mathrm{d}t = \int_{K_0}^{K_1} \mathscr{L}M\,\mathrm{d}K, \tag{37}$$

where at $t = 0$, $K = K_0$ and at the end of the process $t = t_f$ the curvature is equal to its final value $K = K_1$. Now, assuming the length of the plastically deforming zone to be constant during the deformation process, eqn (37) is reduced to

$$E_{\mathrm{CROLL}} = \alpha_1 R_1 \int_{K_0}^{K_1} M(K)\,\mathrm{d}K. \tag{38}$$

For a work-hardening material the state of stress is *continuously moving* along the moment curvature curve from the points A to E so that the plastic energy dissipation E is proportional to the area under this curve.

Present analysis

The assumed kinematic model consists of a discrete plastic hinge moving with velocity V with respect to material points. The rate of plastic work is defined as a product of a bending moment and an angular velocity $[\dot{\theta}]$ in the hinge

$$\dot{E} = M[\dot{\theta}]. \tag{39}$$

Using the condition of kinematic continuity $[\dot{\theta}] + V[K] = 0$ (see, for example, [23]). Equation

(39) can be transformed to

$$\dot{E} = -MV[K] = MV[K_1 - K_0]. \tag{40}$$

In front of the hinge, the curvature is $1/R_0$ and behind it $1/R_1$. Hence at each stage of the deformation both M and $[K]$ are constant. The only parameter of the process is the variable tangential velocity V.

The total plastic work is equal to the time integral of eqn (40):

$$E_{W-B} = \int_0^{t_f} \dot{E}\, dt = M[K_1 - K_0] \int_0^{t_f} V(t)\, dt. \tag{41}$$

The time integral of the tangential velocity is the distance traveled by the hinge $\mathscr{L} = R_1\alpha_1$. Thus the final expression for the plastic energy becomes

$$E_{W-B} = \alpha_1 R_1 M[K_1 - K_0]. \tag{42}$$

For a work-hardening material, the bending moment corresponding to the final curvature K_1 is $M(K_1)$. Consequently, the state of stress is sitting at the point E throughout the entire deformation process. The corresponding plastic work is represented by the rectangular area which is generally greater than the trapezoidal area.

In the limiting case of a rigid-perfectly plastic material $M(K) = \text{const} = M_0$. It is easy to see that eqn (38) reduces then to eqn (42). The plastic energies calculated using Croll's and the present model are the same. With increasing the work-hardening parameter, Croll's formula tends to underestimate the plastic energy dissipation. This is illustrated in Fig. 12 were a nondimensional propagation pressure is plotted versus the so-called buckle propagation parameter m. For aluminum pipes with $h/D = 1/20$, the propagation parameter is of the order $m = 0.01$, so that the difference between the two solutions is insignificant. Mild steel pipes of $W/D = 1/20$ are characterized by $m \cong 0.08$ for which the same difference is not negligible.

We can conclude that both the present and Croll's approaches are theoretically sound. The final solutions are however different since plastic work is path dependent and the assumed paths are not the same. A final test of any approximate analytical solution must be in the experimental verification. Both solutions describe accurately the final shape of the

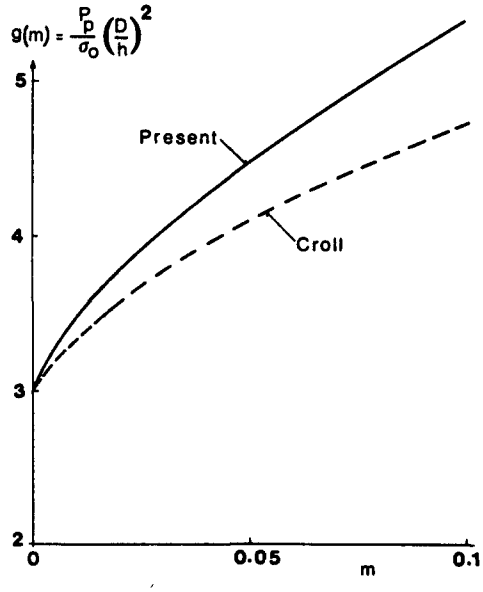

Fig. 12. Comparison of the present theoretical result for propagation pressure with that of Croll[8]

collapsed tube. However, our solution better fits the test points for the minimum propagation pressure. Therefore, we recommend our formula for design purposes.

REFERENCES

1. A. C. Palmer and J. H. Martin, Buckle propagation in submarine pipelines. *Nature* **1**, 46–48 (1975).
2. R. Mesloh, T. G. Johns and J. E. Sorenson, The propagating buckle. *Proc. Boss 76* **1**, 787–797 (1976).
3. S. Kyriakides and C. D. Babcock, Experimental determination of the propagation pressure of circular pipes. *ASME J. Pressure Vessel Technol.* **103**, 328–336 (1981).
4. S. Kyriakides and C. D. Babcock, Buckle propagation phenomena in pipelines, Collapse: The buckling of structures in theory and practice. *Proceedings of the IUTAM Symposium on Collapse, London, August 1982* (Edited by J. M. T. Thomson and G.-W. Hunt), pp. 75–91. Cambridge University Press (1983).
5. S. Kyriakides, C. D. Babcock and D. Elyada, Initiation of propagating buckles from local pipeline damages. *Proceedings of the Energy Sources Technology Conference*, ASME, Houston, Texas, 1983, pp 471–480; also *ASME J. Energy Resources Technol.* **106**, 79–87 (1984).
6. E. Chater and J. W. Hutchinson, On the propagation of bulges and buckles. Harvard University Report No. MECH-44 (June 1983).
7. S. Kyriakides, M.-K. Yeh and D. Roach, On the determination of propagation pressure of long circular tubes. *J. Pressure Vessel Technol., Trans. ASME* **106**, 150–159 (1984).
8. J. G. A. Croll, Buckle propagation in marine pipelines. *Proceedings of the Fourth International Offshore Mechanics and Arctic Engineering Symposium*, Dallas, 1985, pp. 499–507.
9. J. G. A. Croll, Analysis of buckle propagation in marine pipelines, *J. Construct. Steel Res.*, to be published.
10. S. R. Reid and T. Y. Reddy, Effect of strain hardening on the lateral compression of tubes between rigid plates. *Int. J. Solids Struct.* **14**, 213–225 (1978).
11. T. Wierzbicki and W. Abramowicz, On the crushing mechanics of thin walled structures. *J. Appl. Mech.* **50**, 727–734 (1983).
12. W. Abramowicz and A. Sawczuk, On plastic inversion of cylinders. *Res. Mech. Lett.* 525–530 (1981).
13. T. Wierzbicki and S. U. Bhat, A moving hinge solution for axisymmetric crushing of tubes. Technical report, Department of Ocean Engineering, MIT, February, 1985.
14. S. Kyriakides and C. D. Babcock, Prediction of wet buckles in offshore pipeline. *Proceedings of the Marine Technology 1980 Conference*, Washington, D.C., October 1980, pp. 439–444.
15. N. Jones, Plastic failure of ductile beams loaded dynamically. *J. Eng. Ind. Trans. ASME* 131–136 (February 1976).
16. T. Wierzbicki, C. Chryssotomidis and C. Wiernicki, Rupture analysis of ship plating due to hydrodynamic wave impact. *Proceedings of the Ship Structures Symposium*, 1984.
17. J. Strating, A survey of pipelines in the North Sea incidents during installation, testing and operations. *Proceedings of the Offshore Technology Conference*, OTC 4069, 1981, pp. 25–32.
18. R. J. Brown, Pipelines can be designed to resist impact from dragging anchors and fishing boards. *Proceedings of the Offshore Technology Conference*, OTC 1570, 1972, pp. 579–580.
19. C. K. W. Tam and J. G. A. Croll, Buckle initiation in damaged subsea pipelines. Presented at the 4th annual Pipeline Symposium, Energy-sources Technology Conference and Exhibition, Dallas, February 17–21, 1985.
20. J. G. de Oliveira, T. Wierzbicki and W. Abramowicz, Plastic behavior of tubular members under lateral concentrated loading. Det norske Veritas Report No. 82-0708 (1982).
21. G. Augusti, Mode approximations for rigid-plastic structures supported by an elastic medium. *Int. J. Solids Struct.* **6**, 809–827 (1970).
22. S. U. Bhat and P. C. Xirouchakis, Rigid-plastic analysis of floating plates. MIT Dept. of Ocean Engineering, Report No. 84-11 (*ASCE J. Eng. Mech. Div.*, to be published).
23. H. G. Hopkins, On the behaviour of infinitely long rigid plastic beams under transverse concentrated load *J. Mech. Phys. Solids* **4**, 38–52 (1955).

APPENDIX A

The deformed ring shape shown in Fig. 5(b) consists of two straight line segments and two circular arcs. The perimeter of the ring is assumed to remain constant; therefore, the radius r of the circular arc is related to half the length of the linear segment ξ by

$$r/R = 1 - 2\xi/\pi R. \tag{A1}$$

From the geometry of the deformed ring,

$$D^*/D = r^*/R, \tag{A2}$$

where r^* is the value of r corresponding to a given D^*.

Plastic energy dissipation takes place at the four traveling hinges A, B, C, D and also throughout the arcs of radius r which undergo uniform change of curvature at any instant. The rate of energy dissipation has now an additional term due to the continuously deforming region:

$$\dot{E}_{\text{int}} = \sum_{i=1}^{4} |M_i[\Omega]_i| + \int_L M\dot{K}\, dl, \tag{A3}$$

where the first term on the right-hand side has the same interpretation as in eqn (7), L is the total of the length

continuously deforming region, and $\dot{K}$ is the rate of change of curvature. Differentiating $K = 1/r$, one gets $\dot{K} = -\dot{r}/r^2$. Rigid-perfectly plastic material is assumed, so that $|M_i| = |M| = M_0$ Using eqn (8) to determine $[\Omega]$, we can write

$$\dot{E}_{\text{int}} = 4M_0(V/r) + |2\pi r M_0(-\dot{r}/r^2)|, \tag{A4}$$

where $V = \mathrm{d}\xi/\mathrm{d}t$ is the velocity of the material past the hinges. Using eqn (A1), we get $V = -\pi\dot{r}/2$, which simplifies eqn (A4) to

$$\dot{E}_{\text{int}} = -4\pi M_0(r/r). \tag{A5}$$

It is trivial to compute the area enclosed by the deformed ring

$$A = \pi r^2 + 4r\xi = 2\pi Rr - \pi r^2. \tag{A6}$$

According to the hypothesis proposed in the body of the paper,

$$P_l = \frac{\int_0^{t^*} \dot{E}_{\text{int}}\,\mathrm{d}t}{\pi R^2 - A^*} = \frac{-4\pi M_0 \int_R^{r^*} (\mathrm{d}r/r)}{\pi(R-r^*)^2},$$

which gives (A7)

$$P_l = \frac{4M_0 \ln(R/r^*)}{(R-r^*)^2}.$$

We now need a solution for P_p according to this model. Using the fact that propagation pressure is the minimum initiation pressure, we minimize P_l given by eqn (A7) with respect to r^* to get

$$P_p = 9.8M_0/R^2. \tag{A8}$$

Combining eqns (A2), (A7) and (A8),

$$\frac{P_l}{P_p} = \frac{0.41 \ln(D/D^*)}{(D/D^*-1)^2}. \tag{A9}$$